Data report: biogenic silica deposition in the eastern equatorial Pacific[1]

Oscar E. Romero[2]

Chapter contents

[1] Romero, O.E., 2013. Data report: biogenic silica deposition in the eastern equatorial Pacific. *In* Pälike, H., Lyle, M., Nishi, H., Raffi, I., Gamage, K., Klaus, A., and the Expedition 320/321 Scientists, *Proc. IODP,* 320/321: Tokyo (Integrated Ocean Drilling Program Management International, Inc.). doi:10.2204/iodp.proc.320321.206.2013
[2] Instituto Andaluz de Ciencias de la Tierra (CSIC-UGR), Avenida de las Palmeras 4, 18100 Armilla-Granada, Spain. oromero@ugr.es

Abstract

Long-time records of biogenic silica (opal) help researchers to evaluate the effects of global climatic, tectonic, and geochemical Cenozoic events on biological paleoproductivity. Integrated Ocean Drilling Program Expedition 321 Site U1337 contains expanded, nearly continuous records of diatomaceous sediment deposited in deep waters of the eastern equatorial Pacific during the Neogene. In this study, the variability of the biogenic silica at Site U1337 is described by examining temporal changes between the latest middle Miocene and the latest Pleistocene. Periods of highest opal content match well the occurrence of diatom-rich, laminated sediment of the early late Miocene and the late Miocene–Pliocene transition. Lowest contents are measured in the middle Miocene.

Introduction

Biogenic silica (opal) produced by diatoms, silicoflagellates, radiolarians, and sponges is a major constituent of marine sediments and an important parameter for geochemical and paleoceanographic studies. Because of the observed links between diatom production and export productivity (Romero and Armand, 2010), biogenic silica is an indicator of the efficiency of the biological pump and export production (Dugdale et al., 1995).

High-resolution records of sedimentary proxies provide insights into fine-scale geochemical and biological responses to climate forcing. In conjunction with shipboard (geophysical/geochemical) measurements, shore-based biogenic silica records allow the high-resolution evaluation of paleoproductivity variations in surface waters and dissolution effects on long timescales. This provides researchers additional data sets that help to evaluate the effect of global climatic, tectonic, and geochemical events that were typical of the Neogene (Cortese et al., 2004) on the regional biological paleoproductivity.

One of the important accomplishments of Integrated Ocean Drilling Program (IODP) Expedition 321 was to recover continuous Neogene sedimentary sections. These represent the only complete Neogene sections in the equatorial Pacific that have high enough sedimentation rates to resolve orbitally forced paleoproductivity cycles (**Pälike et al.,** 2010). To assess changes in (siliceous) paleoproductivity through time, the content of biogenic silica was de-

doi:10.2204/iodp.proc.320321.206.2013

termined in sediment from Site U1337. Our primary target for this and future work at this site is understanding the long-term relationship between the sedimentary signature of biogenic silica and climate and between tectonic and biogeochemical signatures during the Neogene in the eastern equatorial Pacific.

Materials

For this study, we used samples from Holes U1337A (3°50.0065′N, 123°12.3558′W; water depth = 4472.0 m), U1337B (3°50.0067′N, 123°12.3621′W; water depth = 4472.0 m), and U1337C (3°50.0067′N, 123°12.3755′W; water depth = 4478.6 m). Samples for the analysis of biogenic silica were freeze-dried and ground in an agate mortar.

Methodology

All biogenic silica (opal) analyses were conducted at the Center for Marine Environmental Sciences (MARUM; University of Bremen, Bremen, Germany). Opal procedures followed Müller and Schneider (1993), who modified the method originally proposed by DeMaster (1981). The wet-chemical leaching technique involves the extraction of biogenic silica using hot alkaline solutions, measurements by using inductively coupled plasma–emission spectroscopy (ICP-ES) coulometry, and correction for nonbiogenic silica released from coexisting aluminosilicates and quartz (Müller and Schneider, 1993).

An important advantage of the automated extraction method used in our measurements is that the method provides complete biogenic silica recovery and corrects for the nonbiogenic silica. The method determines only one element (Si), and no assumption with respect to the sediment composition has to be made (Müller and Schneider, 1993). A weak point in the manual technique is that the linear slope and the extrapolated intercept values are based on only a few measurements (usually three or four). Based on replicate measurements of silicon standard solutions, the precision of the analytical system is better than +0.5% (Müller and Schneider, 1993).

Results

The results are represented in Figure **F1.** A total of 364 measurements were conducted on samples from between 4.2 and 258.8 meters below seafloor (mbsf) (Table **T1**). According to the ship-based stratigraphic model, this interval extends from the latest middle Miocene to the latest Pleistocene (**Pälike et al.,** 2010). The data show relatively large variability: biogenic silica contents across all samples vary between 1.9 and 69.5 wt% (average = 16.0 wt%) (Table **T1**).

Fine-scale variability occurs throughout the studied interval. Although measurements between the uppermost part of the sediment column at Site U1337 downhole to ~260 mbsf are not completely continuous, some general trends are recognized. Highest contents occur between 228 and 185 mbsf (uppermost interval of the late Miocene) and 108 and 93 mbsf (corresponding to the Miocene–Pliocene transition). Both intervals of highest biogenic silica content match the occurrence of diatom-rich laminations at Site U1337 (**Pälike et al.,** 2010) (Fig. **F1**). Following the low values between 170 and 165 mbsf, biogenic silica content increases uphole until 110 mbsf. The upper half of the lower Pliocene contains more biogenic silica in than during the lower half, and the range of biogenic silica during the Pleistocene resembles that of the uppermost Pliocene. The lowest biogenic silica contents occur in the uppermost middle Miocene (254–240 mbsf).

Future work on Site U1337 will include filling the gaps (Fig. **F1**), extending the measurements downhole to the lowermost Neogene, applying an age model, calculating the mass accumulation rate of biogenic silica, and evaluating the spectral evolution. Additionally, we will compare our results to other records from Site U1337, and from high latitudes, in order to establish possible interhemispheric connections.

Acknowledgments

This research used samples provided by the Integrated Ocean Drilling Program (IODP). Marco Klann (MARUM) performed the analyses. Financial support was provided by the Spanish Scientific Research Council (CGL2007-31136-E/BTE). Reviewer comments from Julia Shackford and an anonymous reviewer are deeply appreciated.

References

Cortese, G., Gersonde, R., Hillenbrand, C.-D., and Kuhn, G., 2004. Opal sedimentation shifts in the world ocean over the last 15 Myr. *Earth Planet. Sci. Lett.,* 224(3–4):509–527. **doi:10.1016/j.epsl.2004.05.035**

DeMaster, D.J., 1981. The supply and accumulation of silica in the marine environment. *Geochim. Cosmochim. Acta,* 45(10):1715–1732. **doi:10.1016/0016-7037(81)90006-5**

Dugdale, R.C., Wilkerson, F.P., and Minas, H.J., 1995. The role of a silicate pump in driving new production. *Deep-Sea Res., Part 1,* 42(5):697–719. **doi:10.1016/0967-0637(95)00015-X**

Müller, P.J., and Schneider, R., 1993. An automated leaching method for the determination of opal in sediments and particulate matter. *Deep-Sea Res.,* 40:425–444.

Pälike, H., Nishi, H., Lyle, M., Raffi, I., Gamage, K., Klaus, A., and the Expedition 320/321 Scientists, 2010. Expedition 320/321 summary. *In* Pälike, H., Lyle, M., Nishi, H., Raffi, I., Gamage, K., Klaus, A., and the Expedition 320/321 Scientists, *Proc. IODP,* 320/321: Tokyo (Integrated Ocean Drilling Program Management International, Inc.). **doi:10.2204/iodp.proc.320321.101.2010**

Romero, O.E., and Armand, L.K., 2010. Marine diatoms as indicators of modern changes in oceanographic conditions. *In* Smol, J.P., and Stoermer, E.F. (Eds.), *The Diatoms: Applications for the Environmental and Earth Sciences* (2nd ed.): Cambridge (Cambridge Univ. Press), 373–400.

Initial receipt: 2 June 2012
Acceptance: 17 October 2012
Publication: 18 January 2013
MS 320321-206

Figure F1. Plot of biogenic silica (opal) content vs. depth, Site U1337. Yellow areas define the downhole occurrence of diatom-rich laminated oozes (LDO) (**Pälike et al.,** 2010).

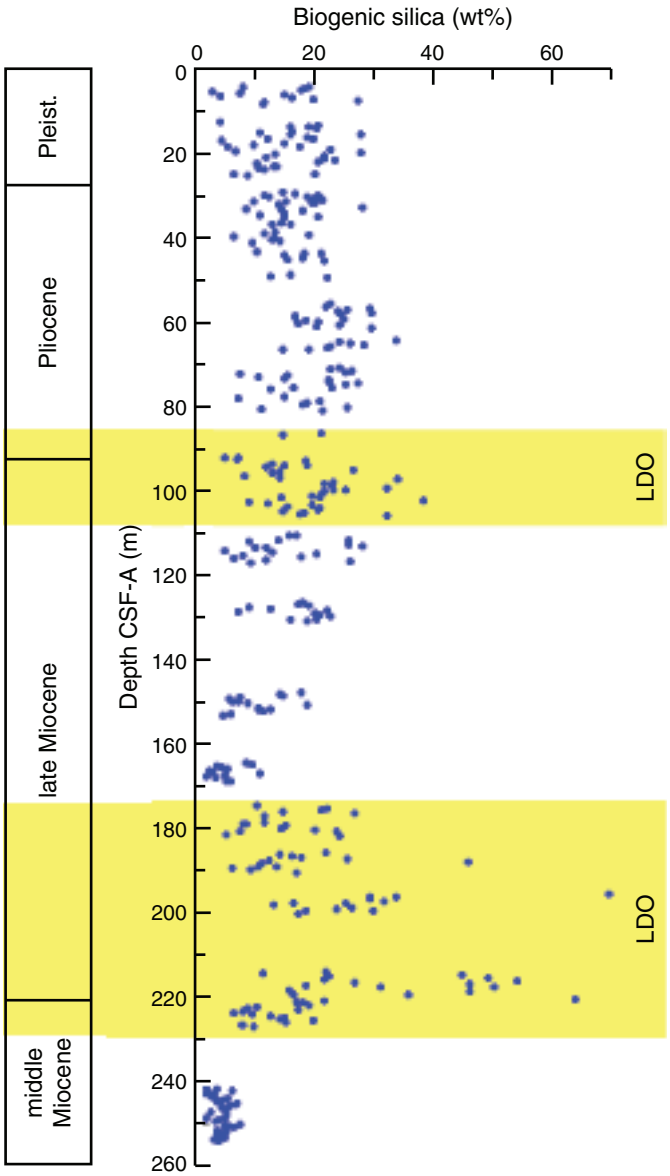

Table T1. Biogenic silica (opal) content, Site U1337. (Continued on next two pages.)

Hole, core, section, interval (cm)	Depth (mbsf)	Biogenic silica (wt%)
321-		
U1337B-1H-3, 70–71	4.16	8.14
U1337B-1H-3, 100–101	4.46	19.06
U1337B-1H-3, 130–131	4.76	18.37
U1337A-2H-3, 130–31	5.05	17.92
U1337A-2H-4, 40–41	5.55	3.06
U1337A-2H-4, 70–71	5.85	7.54
U1337A2-H-4, 100–101	6.15	15.06
U1337A-2H-4, 130–131	6.45	4.33
U1337A-2H-5, 40–41	6.95	16.32
U1337A-2H-5, 70–71	7.25	19.95
U1337A-2H-5, 100–101	7.55	27.28
U1337A-2H-5, 130–131	7.85	11.77
U1337A-2H-6, 40–41	8.35	11.47
U1337A-3H-1, 130–131	12.65	4.32
U1337A-3H-2, 40–41	13.25	20.74
U1337A-3H-2, 70–71	13.55	19.13
U1337A-3H-2, 100–101	13.85	16.11
U1337A-3H-2, 130–131	14.15	20.35
U1337A-3H-3, 40–41	14.75	16.28
U1337A-3H-3, 70–71	15.05	11.00
U1337A-3H-3, 100–101	15.35	16.09
U1337A-3H-3, 130–131	15.65	27.94
U1337A-3H-4, 40–41	16.15	19.04
U1337A-3H-4, 70–71	16.45	20.03
U1337A-3H-4, 100–101	16.75	12.26
U1337A-3H-4, 130–131	17.05	4.63
U1337A-3H-5, 40–41	17.65	15.14
U1337A-3H-5, 70–71	17.95	9.98
U1337A-3H-5, 100–101	18.25	17.65
U1337A-3H-5, 130–131	18.55	5.46
U1337A-3H-6, 40–41	19.15	22.66
U1337A-3H-6, 70–71	19.45	6.85
U1337B-3H-2, 40–41	19.99	27.84
U1337B-3H-2, 70–71	20.29	13.51
U1337B-3H-2, 100–101	20.59	21.78
U1337B-3H-2, 130–131	20.89	12.06
U1337B-3H-3, 40–41	21.49	21.65
U1337B-3H-3, 70–71	21.79	23.60
U1337B-3H-3, 100–101	22.09	20.82
U1337B-3H-3, 130–131	22.39	10.34
U1337B-3H-4, 40–41	22.99	13.16
U1337B-3H-4, 70–71	23.29	13.70
U1337B-3H-4, 100–101	23.59	10.77
U1337B-3H-4, 130–131	23.89	11.71
U1337B-3H-5, 70–71	24.79	20.19
U1337B-3H-5, 100–101	25.09	6.56
U1337B-3H-5, 130–131	25.39	8.92
U1337A-4H-4, 40–41	29.40	14.78
U1337A-4H-4, 70–71	29.70	16.89
U1337A-4H-4, 100–101	30.00	11.73
U1337A-4H-4, 130–131	30.30	12.47
U1337A-4H-5, 40–41	30.90	21.46
U1337A-4H-5, 70–71	31.20	20.08
U1337A-4H-5, 100–101	31.50	19.81
U1337A-4H-5, 130–131	31.80	20.12
U1337B-4H-1, 70–71	30.10	20.65
U1337B-4H-1, 100–101	30.40	18.94
U1337A-4H-1, 130–131	30.70	20.12
U1337B-4H-2, 40–41	31.30	15.44
U1337B-4H-2, 70–71	31.60	9.99
U1337B-4H-2, 100–101	31.90	19.64
U1337B-4H-2, 130–131	32.20	14.00
U1337B-4H-3, 40–41	32.80	28.11
U1337B-4H-3, 70–71	33.10	8.79
U1337B-4H-3, 100–101	33.40	14.54
U1337B-4H-3, 130–131	33.70	18.28
U1337B-4H-4, 40–41	34.30	15.08
U1337B-4H-4, 70–71	34.60	10.92
U1337B-4H-4, 100–101	34.90	20.75
U1337B-4H-4, 130–130	35.20	15.05
U1337B-4H-5, 100–101	36.40	14.53
U1337B-4H-5, 130–131	36.70	16.13
U1337A-5H-2, 130–131	36.90	12.97
U1337B-5H-1, 40–41	38.78	13.44
U1337B-5H-1, 70–71	39.08	11.63
U1337B-5H-1, 100–101	39.38	19.31
U1337B-5H-1, 130–131	39.68	6.71
U1337B-5H-2, 40–41	40.28	13.17
U1337B-5H-2, 70–71	40.58	13.14
U1337B-5H-2, 100–101	40.88	14.26
U1337B-5H-2, 130–131	41.18	9.58
U1337B-5H-4, 40–41	43.28	10.55
U1337B-5H-4, 70–71	43.58	21.34
U1337B-5H-4, 100–101	43.88	18.41
U1337B-5H-4, 130–131	44.18	15.06
U1337B-5H-5, 40–41	44.78	18.08
U1337B-5H-5, 70–71	45.08	15.60
U1337B-5H-5, 100–101	45.38	21.64
U1337A-6H-4, 70–41	48.85	16.09
U1337A-6H-4, 100–101	49.15	12.78
U1337A-6H-4, 130–131	49.45	22.20
U1337A-6H-5, 70–71	50.58	22.36
U1337B-6H-5, 40–41	55.65	22.85
U1337A-7H-1, 70–71	56.32	21.88
U1337A-7H-1, 100–101	56.62	29.57
U1337A-7H-1, 130–131	56.92	25.66
U1337A-7H-2, 40–41	57.52	24.08
U1337A-7H-2, 70–71	57.82	29.74
U1337A-7H-2, 100–101	58.12	24.53
U1337A-7H-2, 130–131	58.42	17.00
U1337A-7H-3, 40–41	59.02	16.88
U1337A-7H-3, 70–71	59.32	25.02
U1337A-7H-3, 100–101	59.62	18.70
U1337A-7H-3, 130–131	59.92	20.76
U1337A-7H-4, 40–41	60.52	17.45
U1337A-7H-4, 70–71	60.82	24.33
U1337A-7H-4, 100–101	61.12	20.37
U1337A-7H-4, 130–131	61.42	29.75
U1337B-7H-4, 40–41	64.43	33.81
U1337B-7H-4, 70–71	64.73	24.31
U1337B-7H-4, 100–101	65.03	26.15
U1337B-7H-4, 130–131	65.33	28.45
U1337B-7H-5, 40–41	65.73	22.87
U1337B-7H-5, 70–71	66.03	22.36
U1337B-7H-5, 100–101	66.33	19.26
U1337B-7H-5, 130–131	66.63	14.72
U1337A-8H-4, 40–41	70.92	24.28
U1337A-8H-4, 70–71	71.22	22.80
U1337A-8H-4, 100–101	71.52	26.28
U1337A-8H-4, 130–131	71.82	25.42
U1337B-8H-3, 40–41	72.37	7.53
U1337B-8H-3, 70–71	72.67	15.50
U1337B-8H-3, 100–101	72.97	10.71
U1337B-8H-3, 130–131	73.27	14.99
U1337B-8H-4, 40–41	73.87	22.52
U1337B-8H-4, 70–71	74.17	22.61
U1337B-8H-4, 100–101	74.47	27.46
U1337B-8H-4, 130–131	74.77	25.31
U1337B-8H-5, 40–41	75.37	22.96
U1337B-8H-5, 70–71	75.67	16.72
U1337B-8H-5, 100–101	75.97	12.71
U1337A-9H-1, 100–101	77.76	15.10
U1337A-9H-1, 130–131	78.06	7.39
U1337A-9H-2, 40–41	78.66	20.97
U1337A-9H-2, 100–101	79.26	19.01
U1337A-9H-3, 130–131	79.56	18.10
U1337A-9H-4, 40–41	80.16	25.54

Table T1 (continued). (Continued on next page.)

Hole, core, section, interval (cm)	Depth (mbsf)	Biogenic silica (wt%)
U1337A-9H-4, 100–101	80.76	11.26
U1337A-9H-4, 130–131	81.06	21.62
U1337B-9H-4, 40–41	86.30	21.24
U1337B-9H-4, 70–71	86.60	14.75
U1337A-10H-4, 40–41	92.03	7.31
U1337A-10H-4, 70–71	92.33	5.12
U1337A-10H-4, 100–101	92.63	7.12
U1337A-10H-4, 130–131	92.93	18.60
U1337A-10H-5, 40–41	93.53	12.91
U1337A-10H-5, 70–71	93.83	15.07
U1337A-10H-5, 100–101	94.13	18.99
U1337A-10H-5, 130–131	94.43	12.01
U1337B-10H-1, 70–71	95.23	26.72
U1337B-10H-1, 100–101	95.53	14.41
U1337B-10H-1, 130–131	95.83	12.94
U1337B-10H-2, 40–41	96.43	8.52
U1337B-10H-2, 70–71	96.73	14.37
U1337B-10H-2, 100–101	97.03	14.41
U1337B-10H-2, 130–131	97.33	33.98
U1337B-10H-3, 70–71	98.13	23.41
U1337B-10H-3, 100–101	98.43	21.78
U1337B-10H-3, 130–131	98.73	22.94
U1337B-10H-4, 40–41	99.33	32.26
U1337B-10H-4, 70–71	99.63	25.35
U1337A-11H-1, 100–101	99.93	23.20
U1337A-11H-1, 130–131	100.23	21.80
U1337A-11H-2, 40–41	100.83	21.31
U1337A-11H-2, 70–71	101.13	19.68
U1337A-11H-2, 100–101	101.43	14.44
U1337A-11H-2, 130–131	101.73	20.92
U1337A-11H-3, 40–41	102.33	38.32
U1337A-11H-3, 70–71	102.63	9.15
U1337A-11H-3, 100–101	102.93	12.27
U1337A-11H-3, 130–131	103.23	19.73
U1337A-11H-4, 40–41	103.83	15.57
U1337A-11H-4, 70–71	104.13	21.10
U1337A-11H-4, 100–101	104.43	20.83
U1337A-11H-4, 130–131	104.73	14.85
U1337A-11H-5, 40–41	105.33	18.42
U1337A-11H-5, 70–71	105.63	17.68
U1337A-11H-5, 100–101	105.93	32.15
U1337A-12H-1, 100–101	110.46	15.84
U1337A-12H-1, 130–131	110.76	17.01
U1337A-12H-2, 70–71	111.56	25.90
U1337A-12H-2, 100–101	111.86	14.02
U1337A-12H-2, 130–131	112.16	9.18
U1337A-12H-3, 40–41	112.76	25.98
U1337A-12H-3, 70–71	113.06	28.12
U1337A-12H-3, 100–101	113.36	10.16
U1337A-12H-3, 130–131	113.66	12.03
U1337A-12H-4, 40–41	114.26	5.19
U1337A-12H-4, 70–71	114.56	13.15
U1337A-12H-4, 100–101	114.86	20.55
U1337A-12H-4, 130–131	115.16	8.07
U1337A-12H-5, 40–41	115.76	17.84
U1337A-12H-5, 70–71	116.06	6.64
U1337A-12H-5, 100–101	116.36	11.98
U1337A-12H-5, 130–131	116.66	26.07
U1337A-12H-6, 40–41	117.26	9.50
U1337B-13H-1, 100–101	126.44	18.12
U1337B-13H-1, 130–131	126.74	17.41
U1337B-13H-2, 40–41	127.34	19.26
U1337B-13H-2, 70–71	127.64	9.09
U1337B-13H-2, 100–101	127.94	12.88
U1337B-13H-2, 130–131	128.24	22.36
U1337B-13H-3, 40–41	128.84	7.46
U1337B-13H-3, 70–71	129.14	20.32
U1337B-13H-3, 100–101	129.44	20.99
U1337B-13H-3, 130–131	129.74	22.86
U1337B-13H-4, 40–41	130.34	16.08
U1337B-13H-4, 70–71	130.64	20.46
U1337B-13H-4, 100–101	130.94	18.94
U1337B-15H-1, 130–131	147.75	17.82
U1337B-15H-2, 40–41	148.35	14.43
U1337B-15H-2, 70–71	148.65	14.80
U1337B-15H-2, 100–101	148.95	7.66
U1337B-15H-2, 130–131	149.25	5.86
U1337B-15H-3, 40–41	149.85	6.43
U1337B-15H-3, 70–71	150.15	7.48
U1337B-15H-3, 100–101	150.45	8.92
U1337B-15H-3, 130–131	150.75	18.80
U1337B-15H-4, 40–41	151.35	10.82
U1337B-15H-4, 70–71	151.65	10.80
U1337B-15H-4, 100–101	151.95	12.82
U1337B-15H-4, 130–131	152.25	11.61
U1337B-15H-5, 40–41	152.85	5.97
U1337B-15H-5, 70–71	153.15	4.71
U1337A-17H-2, 70–71	164.43	8.65
U1337A-17H-2, 100–101	164.73	9.75
U1337A-17H-2, 130–131	165.03	3.68
U1337A-17H-3, 40–41	165.63	4.57
U1337A-17H-3, 70–71	165.93	5.49
U1337A-17H-3, 100–101	166.23	2.38
U1337A-17H-3, 130–131	166.53	3.05
U1337A-17H-4, 40–41	167.13	11.04
U1337A-17H-4, 70–71	167.43	4.97
U1337A-17H-4, 100–101	167.73	1.99
U1337A-17H-4, 130–131	168.03	3.62
U1337A-17H-5, 40–51	168.63	6.07
U1337A-17H-5, 70–71	168.93	5.24
U1337A-18H-1, 100–101	174.56	10.41
U1337A-18H-2, 40–41	175.46	22.37
U1337A-18H-2, 70–71	175.76	21.13
U1337A-18H-2, 100–101	176.06	14.90
U1337A-18H-2, 130–131	176.36	26.86
U1337A-18H-3, 40–41	176.96	11.68
U1337A-18H-4, 40–41	178.46	11.62
U1337A-18H-4, 70–71	178.76	8.07
U1337A-18H-4, 100–101	179.06	8.62
U1337A-18H-4, 130–131	179.36	15.33
U1337A-18H-5, 40–41	179.96	14.57
U1337A-18H-5, 70–71	180.26	20.14
U1337A-18H-5, 100–101	180.56	7.67
U1337A-18H-5, 130–131	180.86	23.92
U1337A-18H-6, 40–41	181.46	5.38
U1337A-18H-6, 70–71	181.76	24.26
U1337A-19H-2, 40–41	185.90	21.89
U1337A-19H-2, 70–71	186.20	14.39
U1337A-19H-2, 100–101	186.50	16.24
U1337A-19H-2, 130–131	186.80	17.99
U1337A-19H-3, 40–41	187.40	25.67
U1337A-19H-3, 70–71	187.70	12.51
U1337A-19H-3, 100–101	188.00	45.90
U1337A-19H-3, 130–131	188.30	11.27
U1337A-19H-4, 40–41	188.90	13.70
U1337A-19H-4, 70–71	189.20	10.80
U1337A-19H-4, 100–101	189.50	6.37
U1337A-19H-4, 130–131	189.80	9.45
U1337A-19H-5, 40–41	190.40	17.01
U1337A-20H-1, 130–131	195.50	69.48
U1337A-20H-2, 40–41	196.10	33.84
U1337A-20H-2, 70–71	196.40	29.49
U1337A-20H-2, 100–101	196.70	29.42
U1337A-20H-3, 40–41	197.30	31.64
U1337A-20H-3, 70–71	197.60	25.45
U1337A-20H-3, 100–101	197.90	16.67
U1337A-20H-3, 130–131	198.20	13.35
U1337A-20H-4, 40–41	198.80	26.47

Table T1 (continued).

Hole, core, section, interval (cm)	Depth (mbsf)	Biogenic silica (wt%)
U1337A-20H-4, 70–71	199.10	23.78
U1337A-20H-4, 100–101	199.40	29.84
U1337A-20H-4, 130–131	199.70	18.73
U1337A-20H-5, 40–41	200.30	17.29
U1337C-6H-1, 70–71	213.95	21.95
U1337C-6H-1, 100–101	214.25	11.39
U1337C-6H-1, 130–131	214.55	44.77
U1337C-6H-2, 40–41	215.15	22.50
U1337C-6H-2, 70–71	215.45	49.26
U1337C-6H-2, 100–101	215.75	21.68
U1337C-6H-2, 130–131	216.05	53.98
U1337C-6H-3, 40–41	216.65	26.80
U1337C-6H-3, 70–71	216.95	46.13
U1337C-6H-3, 100–101	217.25	18.63
U1337D-22H-1, 40–41	217.45	50.11
U1337D-22H-1, 70–71	217.75	31.19
U1337D-22H-1, 130–131	218.35	15.73
U1337D-22H-2, 40–41	218.85	46.05
U1337C-7H-1, 70–71	219.29	35.98
U1337C-7H-1, 100–101	219.59	16.58
U1337C-7H-1, 130–131	219.89	52.90
U1337C-7H-2, 40–41	220.49	63.77
U1337C-7H-2, 70–71	220.79	21.68
U1337C-7H-2, 100–101	221.09	17.24
U1337C-7H-2, 130–131	221.39	18.26
U1337C-7H-3, 40–41	221.99	19.27
U1337C-7H-3, 70–71	222.29	10.52
U1337C-7H-3, 100–101	222.59	8.92
U1337C-7H-3, 130–131	222.89	17.42
U1337C-7H-4, 40–41	223.49	8.20
U1337C-7H-4, 70–71	223.79	6.70
U1337C-7H-4, 100–101	224.09	9.58
U1337C-7H-4, 130–131	224.39	12.69
U1337C-7H-5, 40–41	224.99	15.04
U1337C-7H-5, 70–71	225.29	14.24
U1337C-7H-5, 100–101	225.59	20.03
U1337C-7H-5, 130–131	225.89	15.38
U1337C-7H-6, 40–41	226.49	8.02
U1337C-7H-6, 70–71	226.79	8.17
U1337C-7H-6, 100–101	227.09	9.88
U1337C-9H-2, 40–41	241.46	2.02
U1337C-9H-2, 70–71	241.76	3.91
U1337C-9H-2, 100–101	242.06	6.37
U1337C-9H-2, 130–131	242.36	2.16
U1337C-9H-3, 40–41	242.96	2.01
U1337C-9H-3, 70–71	243.26	3.34
U1337C-9H-3, 100–101	243.56	3.13
U1337C-9H-3, 130–131	243.86	5.70
U1337C-9H-4, 40–41	244.46	4.79
U1337C-9H-4, 70–71	244.76	3.89
U1337C-9H-4, 100–101	245.06	7.17
U1337C-9H-4, 130–131	245.36	6.85
U1337C-9H-5, 40–41	245.96	5.81
U1337C-9H-5, 70–71	246.26	4.45
U1337A-25X-2, 40–41	247.06	5.29
U1337A-25X-2, 70–71	247.36	2.74
U1337A-25X-2, 100–101	247.66	5.24
U1337A-25X-2, 130–131	247.96	5.25
U1337A-25X-3, 40–41	248.56	1.88
U1337A-25X-3, 70–71	248.86	5.17
U1337A-25X-3, 100–101	249.16	3.97
U1337A-25X-3, 130–131	249.46	3.45
U1337A-25X-4, 40–41	250.06	7.55
U1337A-25X-4, 70–71	250.36	4.95
U1337A-25X-4, 100–101	250.66	5.79
U1337A-25X-4, 130–131	250.96	6.54
U1337B-25H-2, 40–41	251.56	3.86
U1337B-25H-2, 70–71	251.86	5.29
U1337B-25H-2, 100–101	252.16	3.71
U1337B-25H-2, 130–131	252.46	4.72
U1337B-25H-3, 40–41	253.06	4.47
U1337B-25H-3, 70–71	253.36	5.06
U1337B-25H-3, 100–101	253.66	3.27
U1337B-25H-3, 130–131	253.96	4.13
U1337B-25H-4, 40–41	254.56	6.27
U1337B-25H-4, 70–71	254.86	4.13
U1337B-25H-4, 100–101	255.16	3.07
U1337B-25H-4, 130–131	255.46	3.60
U1337A-26X-1, 40–41	254.87	4.65
U1337A-26X-1, 70–71	255.17	4.95
U1337A-26X-1, 100–101	255.47	6.62
U1337A-26X-2, 40–41	256.37	4.12
U1337A-26X-2, 70–71	256.67	4.65
U1337A-26X-2, 100–101	256.97	6.76
U1337A-26X-2, 130–131	257.27	5.46
U1337A-26X-3, 40–41	257.87	4.17
U1337A-26X-3, 70–71	258.17	3.18
U1337A-26X-3, 100–101	258.47	11.83
U1337A-26X-3, 130–131	258.77	4.74